NANOSYSTEMS

COMPONENT HYBRIDIZATION IN THIN GRANULATED C_{60}–Cu NANOCOMPOSITE FILMS

O.P. DMYTRENKO,[1] O.L. PAVLENKO,[1] M.P. KULISH,[1]
M.A. ZABOLOTNYI,[1] M.E. KORNIENKO,[1] V.A. BRUSENTSOV,[1]
V.M. RYBII,[1] E.M. SHPILEVSKYI[2]

[1]**Taras Shevchenko National University of Kyiv, Faculty of Physics**
(64, Volodymyrska Str., Kyiv, Ukraine)

[2]**A.V. Lykov Institute of Heat and Mass Transfer**
(15, P. Brovka Str., Minsk BY-220072, Republic of Belarus)

Thin granulated films of C_{60}–Cu nanocomposite with the Cu contents of 80, 34, and 8 at.% were fabricated with the use of the vacuum codeposition method. The films were annealed at a temperature of 473 K for 10, 20, and 30 h in vacuum. Films with lower Cu contents demonstrated a drastic relative intensity decrease and a broadening of the $A_g(2)$ dipole-active vibrational band in the Raman spectrum, which is sensitive to the charge transfer from metal atoms to C_{60} molecules. Further annealing was accompanied not only by a decrease of this band intensity, but also by an intensity increase and a broadening of the $H_g(8)$ vibrational mode band. Moreover, annealing gave rise to the growth of the triplet radiation emission intensity. Similar processes, but with some delay, also occurred in a granular film with a higher copper content. The transformation of Raman and photoluminescence spectra evidenced the polymerization and the destruction of C_{60} molecules owing to the diffusion of copper atoms into C_{60} crystallites, followed by the chemical interaction between those two components due to the charge transfer from metal atoms to fullerenes.

1. Introduction

Fullerene molecules, including the most widespread ones, C_{60}, preserve their unique geometry- and structure-driven properties in the condensed state. These properties, rather unusual for other substances, allow fullerenes to be widely used in various high-technology branches of engineering, energy saving, nanoelectronics, and medicine. The functional properties of fullerites can be considerably extended owing to phase transformations induced by temperature variation, doping, and external influence.

An example of structural changes in fullerites is their polymerization. It takes place, because, instead of the weak van der Waals interaction between fullerenes (it is characteristic of fullerites synthesized under ordinary conditions), there emerges a covalent one. The polymerized state of fullerites can be obtained rather simply by squeezing them at temperatures much higher than room temperature. Depending on the squeezing magnitude and the temperature, various structures emerge in fullerites in the phase equilibrium state. Those structures result from a distortion of the initial solid phase, which is characterized by an fcc lattice at room temperature. A chemical bond of the type [2+2]-cycloaddition can arise along one direction – most likely, along the (001) one, – whereas such an interaction is absent in other planes. A selective character of intermolecular [2+2]-cycloaddition also results in a distortion of the initial phase; there emerges a tetragonal structure, in which the distance between the nearest four neighbor molecules decreases. At higher squeezing and temperatures, there emerges a rhombohedral phase. It is characterized by a distortion of the fcc structure owing to the appearance of a strong chemical interaction between six nearest C_{60} molecules in the (111) plane. In addition to the indicated phases, dimers and a squeezed fcc structure may also emerge. The obtained polymerized phases demonstrate a substantial variation of their electric, optical, mechanical, thermodynamic, and other properties [1–8]. At the same time, it should be noticed that the indicated method can be used to produce polymerized phases in bulk C_{60} specimens as well.

Bulk C$_{60}$ fullerites can also be polymerized by doping them with alkaline metals [9–17]. Doping becomes possible owing to a low cohesion energy of metal atoms, which promotes their insertion from the gas phase into the interstitial positions of the fcc structure. Depending on the number of alkaline metal atoms per every C$_{60}$ molecule (they can be located in octahedral and tetrahedral pores), intermediate structures and A$_x$C$_{60}$ compounds (A = K, Rb, Cs, and x is the number of A atoms per one C$_{60}$ molecule) can be obtained. Every compound is described by a certain crystal structure and characterized by its own set of properties. In particular, the AC$_{60}$ and A$_3$C$_{60}$ compounds have the metallic conductivity, whereas the A$_4$C$_{60}$ and A$_6$C$_{60}$ compounds are insulators. Molecules interact chemically, because the Coulomb interaction is primarily established between the fullerene molecules and alkaline metal atoms as a result of the electron transfer from the latter to the C$_{60}$ molecule. This charge transfer occurs, because alkaline metals are characterized by a low ionization potential, whereas C$_{60}$ molecules, on the contrary, by a high electron affinity.

Films polymerization can also be induced by applying ultra-violet irradiation or bombardment with ionizing particles (γ-photons, electrons, ions, neutrons). It is important that, as the type of the selected irradiation, the energy of bombarding particles, and the exposure dose vary, not only the polymerization mechanisms change from [2+2]-cycloaddition [18–24] to the structure of the "peanut" type [25–29], but also the destruction of C$_{60}$ molecules with the formation of amorphous carbon (α-C) becomes possible. Depending on the ratio between the polymerized phase and amorphous carbon in irradiated specimens, the properties of obtained materials vary substantially, which can be reached by affecting the ratio between the nuclear and electron losses of the energy of ionizing particles, when the particles interact with fullerenes [30–35].

The doping of C$_{60}$ films with non-alkaline metal atoms plays a special role in the modification of film properties. Those metals are characterized by a high cohesion energy and a low electron work function. That is why specimens either with granulated C$_{60}$ and metal nanoparticles or with metal atoms located at the interstitial positions of the C$_{60}$ solid phase can be obtained, depending on the doping technique. In every case, we have a charge transfer from metal atoms to C$_{60}$ molecules: across the phase interface in the former case, and from interstitial positions in the latter one. The magnitude of transferred charge is governed, first of all, by the metal type and by the conditions of film fabrication. The hybridization of electron states in molecules and atoms and the

occupation of the lowest unoccupied molecular orbital (LUMO) in C$_{60}$ fullerites give rise to a considerable interaction between atoms and molecules and also affects transport, magnetic, electronic, optical, mechanical, and other properties of composites obtained [36–39].

In this work, optical properties of thin granulated nanocomposite C$_{60}$ films with copper atoms are studied, as well as their dependences on the copper content and the C$_{60}$–Cu film annealing conditions. The optical properties are researched using photoluminescence and Raman scattering techniques.

2. Experimental Technique

Single-layer copper–fullerene (Cu–C$_{60}$) films were deposited using the simultaneous evaporation of copper atoms in vacuum and the sublimation of fullerene C$_{60}$ molecules obtained from two sources. Films were deposited onto preliminarily oxidized silicon wafers with the (100) surface orientation. Various concentrations of components were driven by varying the rate of copper atom evaporation. Specimens with Cu contents of 80, 34, and 8 at.% were selected for researches. The film morphology was studied with the help of scanning electron microscopy. Vibrational and electron spectra were studied in the framework of the Raman scattering and photoluminescence methods with the use of an Ar laser with an excitation wavelength of 514.5 nm, the power of which did not exceed 2 W/cm^2 to avoid photopolymerization effects.

3. Experimental Results and Their Discussion

The results of X-ray photoemission spectroscopy and high-resolution electron energy loss spectroscopy researches [42] of C$_{60}$ films deposited on metal substrates testify that substrate atoms, similarly to alkaline metal atoms, give their electrons to C$_{60}$ molecules. These electrons occupy the LUMO and change the configurations of HOMO and HOMO-1 energy states [43]. For instance, in the case of precious metals, it was shown that, for Cu, the charge transfer amounts to 1.8 electrons per one C$_{60}$ molecule [44, 45]. The modification of the C$_{60}$ charge state stimulates a redistribution of the charge density in the LUMO and HOMO bands, and, in turn, at single and double bonds between carbon atoms in those molecules. As the scanning tunnel microscopy measurements demonstrate [46], the electron state in the LUMO band is mainly localized at the single bonds of C$_{60}$ pentagons, whereas the HOMO-charge distribution is mainly concentrated at the double bonds of hexagons.
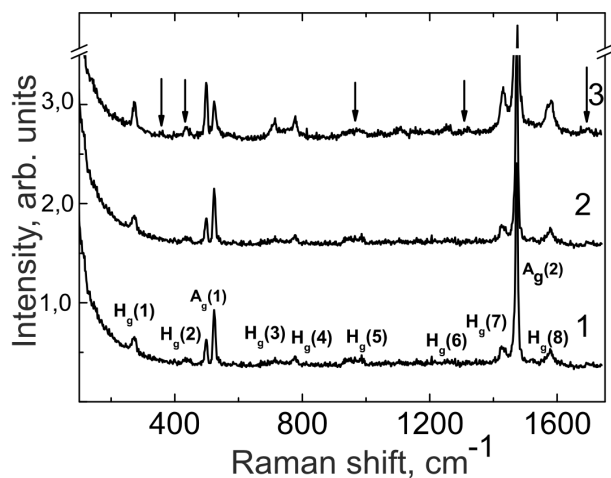
Fig. 1. Raman scattering spectra for granulated C_{60}–Cu films with Cu contents of 8 (*1*), 34 (*2*), and 80 at.% (*3*). The film thickness $d = 100$ nm, the excitation wavelength $\lambda = 514.5$ nm, substrate Si(100)

The increase of charge density at double and single bonds leads to a modification of their lengths, which manifests itself in the shifts of vibrational mode frequencies, which are sensitive to the variations of bond lengths. Tangential vibrational modes react to the charge transfer especially strongly; for instance, these are the modes $A_g(2)$ and $H_g(8)$, which are dipole-active at Raman scattering and located at higher frequencies. It is important that, as the charge density increases, the double bond length becomes elongated from 1.39 to 1.43 Å, whereas the single bond length, on the contrary, becomes shortened from 1.45 to 1.43 Å, which results in that the frequencies of vibrational modes that correspond to different bond types shift in different directions. In the case where the mode is determined by two bond types, it responds to the charge transfer insignificantly, because the contributions made by different bond types compensate each other.

Hence, at the C_{60}–metal interface, similarly to what takes place, when alkaline metal atoms are located in the C_{60} bulk, there is a charge transfer from metal atoms to fullerenes, which results in a shift of dipole-active vibrational modes. For instance, when solid C_{60} is doped with alkaline metal atoms, the totally symmetric pentagonal pinch mode $A_g(2)$ is softened by 3 cm^{-1}, provided that a single electron is transferred to the molecule. In the case of A_3C_{60} and A_6C_{60} compounds, when three and six, respectively, electrons are transferred to a fullerene, the corresponding shifts enlarge proportionally [23, 24].

An analogous situation is observed for the fullerene–metal interface in granulated films, in which the magni-

tude of charge transferred and the hybridization between the electron states of C_{60} molecules and metal atoms depend considerably on the metal content and the conditions of component deposition. Note that, owing to substantial values of cohesion energy for nonalkaline metals, the mutual deposition of C_{60} molecules and metal atoms is accompanied by the formation of granulated films, in which the dimensions of C_{60} and metal granules fall, as a rule, in the limits from 10 to 50 nm. The both indicated factors substantially affect the granular dimensions, the latter governing the diffusion of metal atoms into C_{60} granules and the electron distribution over the energy levels [49]. In its turn, this circumstance affects the charge densities in both fullerene and metal nanogranules.

In Fig. 1, the spectra of Raman scattering for granulated C_{60}–Cu films with Cu contents of 80, 34, and 8 at.% are exhibited. It is evident that, for C_{60}:Cu films, the spectrum mainly coincides with the corresponding spectrum for pure C_{60}, which is characterized by two totally symmetric vibrational modes of type A_g ($A_g(1$–$2)$) at the frequencies of 497 and 1469 cm^{-1}, and eight modes of type H_g ($H_g(1$–$8)$) at the frequencies of 270, 433, 709, 773, 1103, 1253, 1424, and 1576 cm^{-1} [1]. An increase of the Cu atom number per one C_{60} molecule results in a considerable reduction of the intensities of vibrational modes $A_g(1)$ and $A_g(2)$ (see curve 2 in Fig. 1). At the same time, a subsequent increase of the copper atom content to 80 at.% brings about a spectrum that is typical of pure C_{60} [1]. Moreover, the bands of all vibrational modes become amplified, and there appear additional scattering bands at about 360, 430, 968, 1318, and 1695 cm^{-1} (curve *3* in Fig. 1).

It is evident that, if the concentration of copper atoms is low, the number of metal granules is small, so the metal atoms affect the behavior of fullerene vibrational modes insignificantly. Their influence extends only upon the first layer of molecules, which form the metal–C_{60} interface [50]. Despite that this monolayer can even become metallic as a result of charge transfer and LUMO filling, a small number of C_{60} molecules hybridized with the metallic surface apparently do not play an appreciable role, in comparison with the total number of fullerenes that do not interact with metals.

At the same time, an increase of the Cu content leads to a larger number of granules with small dimensions, which is accompanied by the appearance of a considerable number of interfaces, the charge transfer through which results in the emergence of a significant amount of molecules bonded with metals owing to the ionic or donor–acceptor interaction. In Fig. 2, a decomposi-
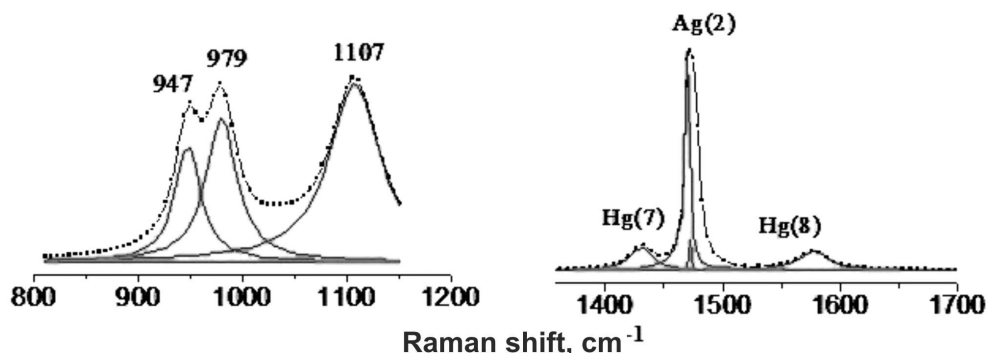
Fig. 2. Decomposition of the Raman spectrum for a C_{60}–Cu film with a Cu content of 34 at.% after deposition into the bands of vibrational modes $H_g(7)$, $A_g(2)$, and $H_g(8)$

tion of the Raman spectrum into possible components is shown in the frequency interval, where the bands of vibrational modes $H_g(7)$, $H_g(8)$, and $A_g(2)$, which are the most sensitive to the charge transfer, are located. Not only a reduction of the relative intensity of line $A_g(2)$ is observed, but also the appearance of its components, which can be a consequence of the shift of this vibrational mode as a result of the charge transfer, as well as of the C_{60} structure polymerization. This polymerization (it is characterized by the emergence of dimers and, probably, more complicated phases) is a manifestation of the partial diffusion of Cu atoms into the region of C_{60} granules at the deposition stage. One may not exclude that the polymerization is more inherent to the layers located closer to the phase interface, being a consequence of the hybridization of molecules and atoms near this surface. [2+2]-cycloaddition remains to be the mechanism of intermolecular interaction, as it was for other cases of polymerization. It is invoked by the hybridization between fullerene sp-states and metal d-states, which results in the chemical interaction between metal atoms and C_{60} molecules. Such strong interaction is evidenced by a considerable reduction of the $A_g(2)$ mode intensity, which becomes possible in the case of molecular destruction; the latter is observed, for example, under high-energy irradiation at large exposure doses [30]. The destruction is accompanied by a growth of the intensity in the interval of vibrational mode $H_g(8)$, i.e. in the range of tangential vibrational mode E_g of amorphous carbon (α-C).

An absolutely different form is inherent to the Raman scattering spectrum for the granulated composite with a copper content of 80 at.%. It is a result of the surface amplification of Raman scattering by C_{60} molecules. Such an amplification may occur owing to the formation of granulated metal nanoparticles in the C_{60} matrix, the dimensions of which are enough for the high-

strength local fields to be created owing to the surface plasmon resonance. The interaction of those fields with scattered waves provides an appreciable growth of the band intensities for all vibrational modes. The charge-transfer-induced distortion of C_{60} molecules is insignificant, which may be associated with the low diffusion of copper atoms from metal granules into the C_{60} matrix bulk. At the same time, the appearance of new dipole-forbidden peaks and the shifts of Raman bands testify to the emergence of hybridization between C_{60} molecules and metal atoms at the phase interface, which is connected with charge transfer.

The granulated particles are characterized by a developed surface, and, like metal islands deposited onto the C_{60} surface [49], they promote the diffusion of copper atoms into the C_{60} bulk. In both the amorphous C_{60} matrix and the crystalline C_{60} phase, the diffused copper atoms occupy positions the most beneficial energetically (in crystals, these are octahedral and tetrahedral voids), from which the charge transfer to C_{60} molecules takes place. Due to this charge transfer, as in the case of alkaline metals, there emerges a chemical interaction between ligands and C_{60} molecules, which, in turn, favors the emergence of an intermolecular interaction giving rise to the polymerization and, probably, to the destruction of C_{60} molecules.

An enhancement of the atomic diffusion can evidently be obtained by the annealing of doped films even at slightly elevated temperatures, because the activation energy of the metal atom diffusion is low, if the intermolecular space dimensions are considerable. Figure 3 exhibits the variation of Raman spectra for a nanocomposite with a copper content of 34 at.% after the annealing at a temperature of 473 K for 10, 20, and 30 h. Note that appreciable changes in the spectrum take place already after the 10-h annealing. These changes are observed in the whole spectral range of dipole-allowed
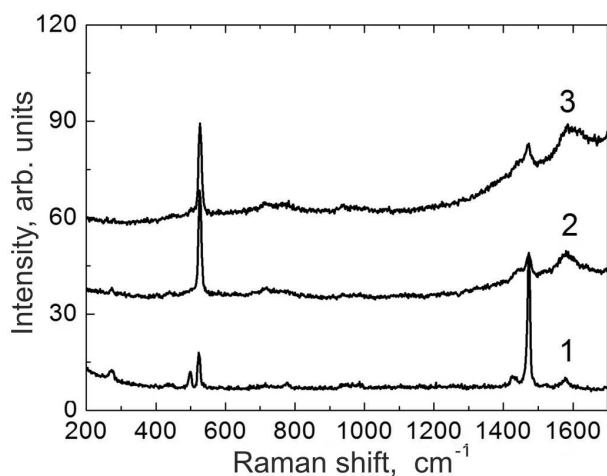
Fig. 3. Raman scattering spectra for C_{60}–Cu films with a Cu content of 34 at.% annealed at a temperature of 473 K for 10 (*1*), 20 (*2*), and 30 h (*3*)

vibrational modes and especially in the range of vibrational modes $H_g(7)$, $A_g(2)$, and $H_g(8)$, which are the most sensitive to the charge transfer and structural changes, including the destruction of C_{60} molecules as a result of the strong interaction with metals. Attention is attracted by an increase of the Raman scattering background in the range of tangential modes as the annealing time grows. In addition, mode $A_g(2)$ strongly broadens out and almost totally overlaps with mode $H_g(7)$; its intensity drastically diminishes to the values, at which the intensity of band $A_g(2)$ not only becomes equal to, but even less than that of peak $H_g(8)$. The indicated reconstruction of the spectrum testifies to a strong distortion of C_{60} molecules, which is a consequence of substantial modifications of the charge density at double and single bonds in fullerenes arising owing to the charge transfer from Cu atoms to C_{60}. It is these modifications of the charge density in the HOMO and LUMO states that affect the elongation of double bonds and the shortening of single ones, which govern the molecular symmetry and, accordingly, the behavior of the vibrational spectrum.

It is worth noting that the diffusion of metal atoms into the matrix with C_{60} brings about not only the destruction of C_{60} molecules and the formation of the α-C phase, which manifests itself in a fading of mode $A_g(2)$ and a growth of the intensity of mode E_g of amorphous carbon, but also more complicated structural transformations in C_{60} fullerites. The presence of such transformations can be seen from the decomposition of $H_g(7)$, $A_g(2)$, and $H_g(8)$ vibrational mode bands into their components at various annealing times (see Fig. 4). At the same time, the shifted bands, which correspond to the

dimerization and more complicated orthorhombic and other structures, have low intensities. Most probably, it is a manifestation of the fact that the majority of C_{60} molecules in the synthesized granules in films, where the polymerization is only partially confined to the dimer formation, are in a disordered state.

Similar modifications are also observed for the specimen with a high Cu content of 80 at.%; however, they are slowed down there. In particular, even after the 20-h annealing at a temperature of 473 K, the picture of the enhanced Raman scattering survives, and a considerable relative decrease of peak intensities with respect to that of band $H_g(8)$ is observed only after the 30-h annealing (see Fig. 5). We may suppose that, in such specimens with large Cu granules, a high cohesion energy constrains metal atoms from the diffusion into C_{60} granules and, consequently, the interaction between molecules and atoms is restricted only near the phase interface. In the C_{60} bulk, owing to a small number of diffusing atoms, the influence on fullerenes is insignificant, but it does take place and increases, if the annealing time grows.

It is evident that the symmetry variation of C_{60} molecules owing to the charge transfer from metal atoms is accompanied by a transformation of the photoluminescence spectrum. In the case of low temperatures (lower than 15 K), the spectrum of the bulk luminescence of C_{60} crystals is a combination of two bands centered at 734 and 684 nm [51]. The band at 734 nm corresponds to the broadband luminescence associated with non-uniformly broadened transitions from a deep X-trap. This trap corresponds to an excited Frenkel exciton with lowered symmetry that is delocalized in the space between two adjacent molecules located either near a vacancy in the crystal or near another defect, which inserts a structure disordering.

The band at 734 nm is also characteristic of crystals at room temperature. It is a high-energy luminescence band with a maximum at 1.69 eV, which is related to the bulk radiation emission of fullerene. In the range of lower energies, this band overlaps with the radiation caused by the presence of X-traps in solid C_{60}. Those traps may be defects of physical or chemical origin, which are located at the site next to the given molecule and violate the translational symmetry in the lattice. At the polymerization, the radiation band shifts toward the red-wave range and broadens in comparison with that for a non-polymerized specimen.

For C_{60} fullerene films, in which the majority of molecules are in the amorphous state, with separate inclusions of crystalline nanoparticles about 40 nm in di-
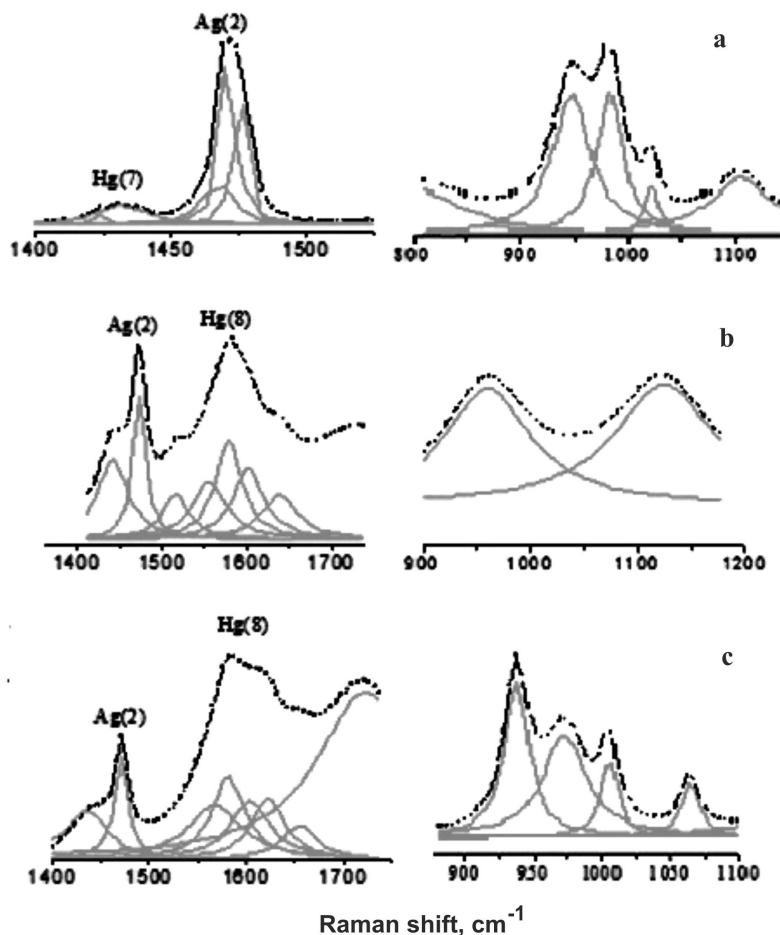
Fig. 4. Decomposition of the Raman spectrum for a C_{60}–Cu film with a Cu content of 34 at.% annealed at a temperature of 473 K for 10 (*a*), 20 (*b*), and 30 h (*c*) into the bands of vibrational modes $H_g(7)$, $A_g(2)$, and $H_g(8)$

mensions, the luminescence spectrum at room temperature includes two wide unstructured emission bands [52–55]. One of them is high-energy; it is located at about 1.69 eV and corresponds to fluorescence. The other is low-energy; it is observed at about 1.4 eV and belongs to phosphorescence [53, 56]. At the polymerization, the intensity ratio between those bands changes. The ratio depends on the temperature, at which the film luminescence spectra were obtained. In particular, at low temperatures, the intensity of the low-energy band grows with increase of the polymerization degree, which evidences the growth in the number of deep traps or the increase of the quantum yield of triplet emission [54, 55]. When dimers, trimers, and chains are formed at the polymerization and the covalent bonds between molecules emerge, the distance between the molecules and their symmetry decrease in comparison with those for the non-polymerized state. Therefore, the energy
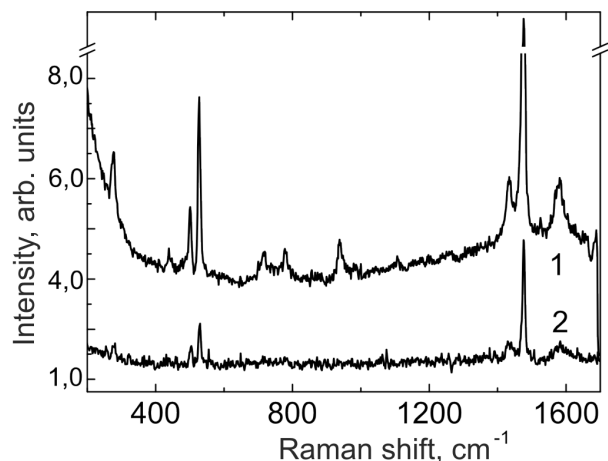

Fig. 5. Raman scattering spectra for C_{60}–Cu films with a Cu content of 80 at.% annealed at a temperature of 473 K for 20 (*1*) and 30 h (*2*)
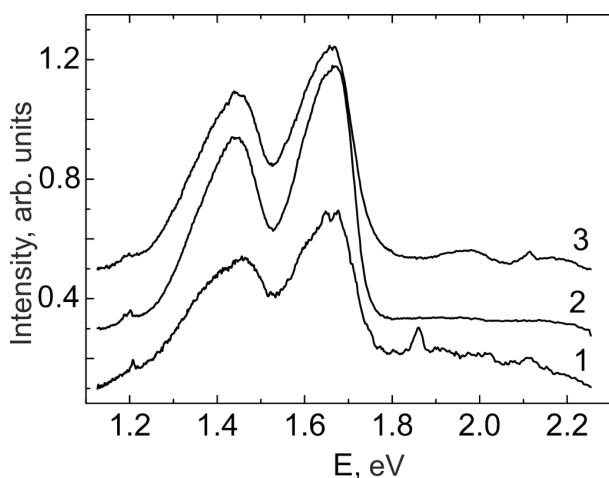
Fig. 6. Photoluminescence spectra for nanocomposite C_{60}–Cu films with a Cu content of 34 at.% after deposition (1) and after annealing at a temperature of 473 K for 10 (2), 20 (3), and 30 h (4). $\lambda = 514.5$ nm, the measurement temperature $T = 77$ K

Fig. 7. Photoluminescence spectra for nanocomposite C_{60}–Cu films with a Cu content of 80 at.% after deposition (1) and after annealing at a temperature of 473 K for 10 (2), 20 (3), and 30 h (4). $\lambda = 514.5$ nm, $T = 77$ K

levels of molecules also decrease. In this connection, a broadening of the energy levels of fullerenes and, accordingly, of local (defect) states, which are responsible for the emission by fullerenes, are observed at the polymerization.

In Fig. 6, the luminescence spectra for a C_{60}–Cu film with a Cu content of 34 at.% obtained after the film deposition and annealing at a temperature of 473 K for 10, 20, and 30 h are depicted. One can see that the luminescence spectrum consists of two wide unstructured bands. By analogy with the results of researches of other similar films, we may assert that the high-energy band at about 1.69 eV is related to the fluorescence of singlet Frenkel excitons captured at a deep X-trap. In this case, the role of the latter is played by a deformed C_{60} molecule in the presence of a vacancy or a Cu atom diffused into the C_{60} matrix either from nano-sized metal granules or in the course of the film deposition. The second wide band appears as a result of the transition from the triplet state of molecules. The high quantum yield of triplet luminescence testifies that a significant number of molecules are in the triplet state after the intercombination transition. The transition of molecules into the triplet state is known to favor the formation of complexes and their mutual binding by covalent bonds. In addition, unlike pure C_{60} films, both bands are very broadened, which testifies to the polymerization, because the latter enhances the spread of fullerene energy levels. In this case, the polymerization mechanism may be less associated with the emergence of [2+2]-cycloaddition between molecules, but it can be related sooner to the emergence
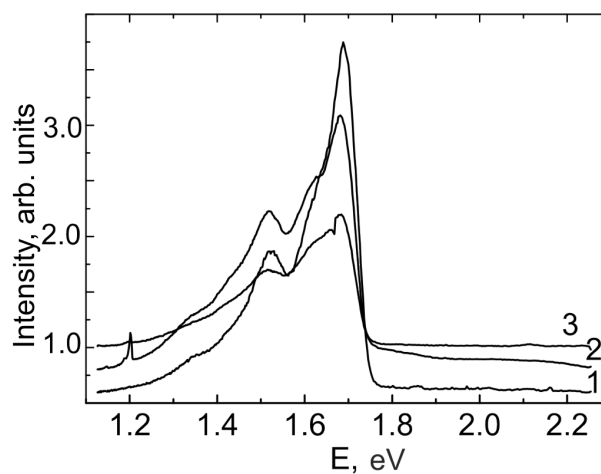
of a chemical interaction of Cu atoms with two neighbor fullerenes. This bond generates, first of all, dimers, in which copper atoms are located between molecules, but the appearance of chain structures is also not excluded.

The annealing of the specimen for 10 and 20 h (Fig. 6, curves 2 and 3) leads to a relative growth of the emission associated with the triplet state. Phosphorescence becomes even larger for the film annealed for 30 h, and the integral intensity becomes almost identical to the relevant value for the fluorescence band. Such an increase of the triplet emission evidences the polymerization growth in disordered films, which is a consequence of the charge transfer from copper atoms that diffuse into C_{60} granules or to neighbor molecules, followed by the establishment of a chemical interaction between them.

The behavior of the luminescence spectrum for films with a high content of copper atoms (80 at.%) is different. For as-deposited films, this spectrum only slightly differs from that for films of pure C_{60}, which is characterized by the rather narrow fluorescence and phosphorescence emission bands at 1.69 and 1.5 eV, respectively (see Fig. 7). We may suppose that, in the course of deposition, when the number of copper atoms is substantial, there occurs the phase segregation with the formation of large enough nanoparticles of both components and the low diffusion of atoms in the C_{60} environment. The atomic diffusion remains insignificant at the annealing for 10 h as well; therefore, the photoluminescence spectrum undergoes little changes in comparison with the initial one. As was in the case of vibrational spectra, the photoluminescence spectrum starts to change only

at the annealing time of 20 h. One can see that the triplet emission intensity considerably grows after this period and continues to increase at the 30-h annealing. It is evident that this growth is a consequence of the formation of complexes with metal atoms owing to the charge transfer from diffused atoms to molecules [57–59]. Therefore, the growth of the metal atom concentration at the deposition does not change the polymerization mechanism, and it remains the same as was at depositing the smaller number of copper atoms, but the polymerization process becomes slower.

4. Conclusions

While doping C$_{60}$ crystals or thin films with alkaline metal atoms characterized by a low cohesion energy, the atomic distribution over the interstitial sites in the lattice is uniform. On the contrary, the codeposition of fullerenes and non-alkaline metals with a high cohesion energy gives rise to the formation of heterogeneous nanocomposites. The latter, depending on the codeposition conditions, consist of separated C$_{60}$ granules and metal atoms with various dimensions and ordering. Such complicated morphology of the films diversely affects their properties, which can change depending on the structure of obtained nanomaterials. A characteristic manifestation of this structure is the charge transfer from metal atoms to C$_{60}$ molecules, which are characterized by a considerable affinity to electrons. The charge transfer occurs both through the phase interface at the granular edge and from metal atoms diffused into the C$_{60}$ matrix. Since the transferred charges are localized at single and double bonds of pentagons and hexagons of molecules and change the LUMO and HOMO states of fullerenes at that, they affect the reduction and the elongation of those bonds. As a consequence, they modify the vibrational spectrum of molecules. First of all, they affect the tangential modes, which become sensitive to the charge transfer and associated structural effects. In addition, the insertion of metal atoms into the C$_{60}$ environment and the establishment of an interaction between them promote the creation of X-traps for Frenkel singlet excitons and influence the quantum yield of the triplet emission. The indicated factors considerably manifest themselves in a transformation of vibrational and photoluminescence spectra, which change depending on the probability of atomic diffusion. The latter is governed by the number of the deposited metal atoms per one C$_{60}$ molecule, annealing of a specimen at elevated temperatures, and polymerization of fullerenes occurring owing

to the chemical interaction between metal atoms and the adjacent C$_{60}$ molecules.

For instance, in codeposited thin granulated films C$_{60}$–Cu with a copper content of 34 at.%, a substantial reduction of the relative integrated intensity of the A$_g$(2) vibrational mode band and its overlapping with the adjacent band of vibrational mode H$_g$(7) are observed even at the deposition stage. The annealing at a temperature of 473 K for 10, 20, and 30 h results in a further decrease of the intensity of this band. At the same time, the intensity of the H$_g$(8) mode band, on the contrary, grows, so that its integrated intensity exceeds that of A$_g$(2) band already at the 20-h annealing. The increase of the annealing time is also accompanied by the growth of the triplet scattering, which may probably testify to the interaction of C$_{60}$ molecules and fullerenes with metal atoms. Since the diffusion of atoms grows with the annealing time, one may suppose that the emergence of a chemical interaction between molecules and atoms is a consequence of the charge transfer from diffused metals to fullerenes. On the one hand, this interaction can promote the polymerization of C$_{60}$ molecules owing to their aggregation with metal atoms and the formation of dimers and chain structures even in the amorphous state of solid C$_{60}$. On the other hand, it can lead to the destruction of molecules, which is evidenced by the growth of the intensity of α–C band within the existence range of vibrational mode H$_g$(8).

For films with a copper content of 80 at.%, the distribution morphology and the dimensions of copper nanoparticles lead to the enhancement of the Raman scattering by strong local fields created by surface plasmon resonances, which arise in these metal nanoparticles. As the annealing time increases, the modifications in the Raman scattering and photoluminescence spectra are similar to those for spectra obtained for films with lower copper contents, but they are realized more slowly. The reason for such a delay in the processes of polymerization and destruction of C$_{60}$ molecules (keeping the mechanism of those effects untouched) is a reduction of the probability of atomic diffusion. This probability is governed by a high cohesion energy typical of large nanoparticles, which are formed in the films under consideration.

1. A.M. Rao, P.C. Eklund, J.-L. Hodeau *et al.*, Phys. Rev. B **78**, 4766 (1997).

2. V.V. Brazhkin, A.G. Lyapin, S.V. Popova *et al.*, Phys. Rev. B **56**, 11465 (1997).

3. V.V. Brazhkin, A.G. Lyapin, Yu.V. Antonov *et al.*, Pis'ma Zh. Eksp. Teor. Fiz. **4**, 328 (1995).

4. V.V. Brazhkin, A.G. Lyapin, and S.V. Popova, Zh. Eksp. Teor. Fiz. **11**, 755 (1996).

5. V.A. Davydov, L.S. Kashevarova, A.V. Rakhmanina *et al.*, Pis'ma Zh. Eksp. Teor. Fiz. **10**, 778 (1996).

6. A.G. Lyapin and V.V. Brazhkin, Fiz. Tverd. Tela **3**, 393 (2002).

7. K.P. Meletov, J. Arvanitidis, S. Assimopoulos *et al.*, Fiz. Tverd. Tela **4**, 601 (2002).

8. V.A. Davydov, L.S. Kashevarova, A.V. Rakhmanina *et al.*, Phys. Rev. B **22**, 14786 (1998).

9. J. Winter, H. Kuzmany, A. Soldatov *et al.*, Phys. Rev. B **9**, 17486 (1996).

10. P. Zhou, K.-A. Wang, Y. Wang *et al.*, Phys. Rev. B **4**, 2595 (1992).

11. G. Dresselhaus, M.S. Dresselhaus, and P.C. Eklund, Phys. Rev. B **12**, 6923 (1992).

12. B. Ha, J.H. Rhee, Y. Li *et al.*, Surf. Sci. **3**, 186 (2002).

13. A.A. Sabouri-Dodaran, Ch. Bellin, M. Marangolo *et al.*, J. Phys. Chem. Solids **5-6**, 1132 (2006).

14. Z.A. Matysina, D.V. Schur, and S.Yu. Zaginaichenko, Carbon **7**, 1369 (2003).

15. M. Riccò, T. Shiroka, M. Belli *et al.*, Phys. Rev. B **15**, 155437 (2005).

16. T. Shiroka, M. Riccò, F. Barbieri *et al.*, Fiz. Tverd. Tela **3**, 498 (2002).

17. S. Saito, K. Umemoto, S.G. Louie *et al.*, Solid State Commun. **5**, 335 (2004).

18. A.M. Rao, P. Zhou, K.-A. Wang *et.al.*, Science **259**, 955 (1993).

19. G.B. Adams, J.B. Page, O.F. Sankey *et al.*, Phys. Rev. B **23**, 17471 (1994).

20. J. Onoe, K. Takeuchi et al., Phys.Rev. Lett. **16**, 2987 (1997).

21. J. Onoe, A. Nakao, and K. Takeuchi, Phys. Rev. B **15**, 10051 (1997).

22. P.C. Eklund, A.M. Rao, Y. Wang *et al.*, Thin Solid Films **257**, 211 (1995).

23. P.C. Eklund, A.M. Rao, P. Zhou *et al.*, Thin Solid Films **257**, 185 (1995).

24. Y. Wang, J.M. Holden, A.M. Rao *et al.*, Phys.Rev. B **7**, 4547 (1995).

25. J. Onoe, T. Hara, and K. Takeuchi., Synth. Metals **121**, 1141 (2001).

26. T.A. Beu, J. Onoe, and A. Hida, Phys. Rev. B **72**, 155416 (2005).

27. J. Onoe, T. Nakayama, M. Aono *et al.*, J. Phys. Chem. Solids **65**, 343 (2004).

28. A. Takashima, J. Onoe, and T. Nishii, J. Appl. Phys. **108**, 033514 (2010).

29. Y. Todaa, S. Ryuzaki, and J. Onoe, Appl. Phys. Lett. **92**, 094102 (2008).

30. F.C. Zavisluk, M. Behar, and D. Fink, Phys. Lett. A **226**, 217 (1997).

31. K.L. Narayanau, M. Yamaguchi, N. Dharmarasu *et al.*, Phys. Rev. B **178**, 301 (2001).

32. R. Kalish, A. Samoiloff, A. Hoffman *et al.*, Phys. Rev. B **24**, 18235 (1993).

33. A.I. Ryabenikov, A.V. Petrov, N.M. Polkovnikova *et al.*, Surf. Coat. Technol. **201**, 8499 (2007).

34. N. Baiwa, A. Ingals, D.K. Avasthi *et al.*, Nucl. Instrum. Methods Phys. Res. B **212**, 233 (2003).

35. K. Narumi, S. Sakai, H. Naramoto *et al.*, Fulleren. Nanotubes Carbon Nanostruct. **14**, 429 (2006).

36. C. Ton-That, A.G. Shard, S. Egger *et al.*, Phys. Rev. B **67**, 155415 (2003).

37. X. Lu, M. Grobis, K.H. Khoo *et al.*, Phys. Rev. B **70**, 115418 (2007).

38. L.-L. Wang and H.-P. Cheng, Phys. Rev. B **69**, 045404 (2004).

39. Z. Zhao, H. Wang, B. Wang *et al.*, Phys. Rev. B **65**, 235 (2002).

40. E. M.Shpilevskii, L.V. Baran, G.P. Okatova *et al.*, in *Diamond Films and Films of Related Materials* (Khark. Fiz.-Tekhn. Inst., Kharkov, 2003), p. 265 (in Russian).

41. E.M. Shpilevskii, in *Diamond Films and Films of Related Materials* (Khark. Fiz.-Tekhn. Inst., Kharkov, 2003), p. 242 (in Russian).

42. M.R.C. Hunt, P. Rudolf, and S. Modesti. Phys. Rev. B **12**, 7882 (1997).

43. B.W. Hoogenboom, R. Hesper, L.H. Tjeng *et al.*, Phys. Rev. B **19**, 11939 (1998).

44. M.R.C. Hunt, S. Modest *et al.*, Phys. Rev. B **15**, 10039 (1995).

45. Z. Zhao, H. Wang, B. Wang *et al.*, Phys. Rev. B **65**, 235 (2002).

46. Y. Maruyama, K. Ohno, and Y. Kawazol, Phys. Rev. B **3**, 2070 (1995).

47. P. Zhou, K.-A. Wang, Y. Wang *et al.*, Phys. Rev. B **4**, 2595 (1992).

48. G. Dresselhaus, M.S. Dresselhaus, and P.C. Eklund, Phys. Rev. B **12**, 6923 (1992).

49. A.F. Hebard, R.R. Ruel, and C.B. Eom, Phys. Rev. B **19**, 14052 (1996).

50. A.V. Talyzin, U. Jansson, and A.V. Usatov, Fiz. Tverd. Tela **3**, 483 (2002).

51. K. Akimoto and K. Kan'no, J. Phys. Soc. Jpn. **2**, 630 (2002).

52. D.J. van den Heuvel, I.Y. Chan, E.J.J. Groenen *et al.*, Chem. Phys. Lett. **233**, 284 (1995).

53. D.J. van den Heuvel, I.Y. Chan, E.J.J. Groenen *et al.*, Chem. Phys. Lett. **231**, 111 (1994).

54. V.A. Karachevtsev, A.Yu. Glamazda, V.A. Pashinskaya *et al.*, Fiz. Nizk. Temp. **8**, 923 (2007).

55. V.A. Karachevtsev, P.V. Mateichenko, N.Yu. Nedbailo *et al.*, Carbon **42**, 2091 (2004).

56. V.V. Kveder, V.D. Negrin, E.A. Shteiman *et al.*, Zh. Eksp. Teor. Fiz. **2**, 734 (1998).

57. T.R. Ohno, Y. Chen, S.E. Harvey *et.al.*, Phys. Rev. B **4**, 2389 (1993).

58. B. Morison, Z. Hu, J.P. Jorgensen *et al.*, Phys. Rev. B. **9**, 6051 (1999).

59. Yu.V. Shevtsov, S.V. Trubin, Yu.V. Shubin *et al.*, Zh. Strukt. Khim. **45**, 77 (2004).

ГІБРИДИЗАЦІЯ КОМПОНЕНТ У ТОНКИХ ГРАНУЛЬОВАНИХ ПЛІВКАХ НАНОКОМПОЗИТА C_{60}–Cu

О.П. Дмитренко, О.Л. Павленко, М.П. Куліш,
М.А. Заболотний, М.Є. Корнієнко,
В.А. Брусенцов, В.М. Рибій,
Е.М. Шпілевський

Р е з ю м е

Методом вакуумного співосадження атомів міді і молекул C_{60} одержано тонкі гранульовані плівки нанокомпозита C_{60}–Cu із вмістом Cu 80 ат.%, 34 ат.% та 8 ат.%. Ці плівки відпалювали при температурі 473 К протягом 10, 20, 30 годин у вакуумі. Для плівок з меншим вмістом атомів міді вже після осадження спостерігається різке зменшення відносної інтенсивності та розширення дипольно активної у раманівському розсіянні коливної моди $A_g(2)$, чутливої до перенесення зарядів від атомів металу до C_{60}. З відпалом зменшення її інтенсивності супроводжується зростанням інтенсивності і розширенням смуги коливної моди $H_g(8)$. Крім того, з відпалом зростає інтенсивність триплетного випромінювання. Аналогічні процеси, але із запізненням, відбуваються у гранульованій плівці з більшим вмістом атомів міді. Трансформація спектрів коливань і фотолюмінесценції вказує на полімеризацію та руйнування молекул C_{60}, яке відбувається за рахунок дифузії атомів міді з гранул у середовище C_{60} з подальшим встановленням між ними хімічної взаємодії за рахунок перенесення зарядів від атомів металу до фулеренів.